Multiscale algorithms for optimal design in materials science

Svetozara Petrova

Department of Mathematics
University of Applied Sciences Bielefeld, Germany

29 September – 3 October, 2014, Dubrovnik

Outline

Outline

Optimal design

Optimization problem and solution methods

Multiscale shape optimization problems

- Microstructural ceramic materials
- Microfluidic biochips

Conclusions

Find "the best" of all possible structural designs within a prescribed objective function $J(\mathbf{u}, \alpha)$ and a set of constraints:

- behavioral (w.r.t. the physical model, typically nonlinear)
- geometrical (manufacturing limitations, typically inequalities)

$\mathbf{u}$ – state variables; α – design variables.

The objective function $J(\mathbf{u}, \alpha)$ can be chosen according to:

- loading (tension, bending, twisting)
- thermal properties (shock resistance)
- technological constraints (minimal weight)
- economical constraints (cheapness)

Three types of structural optimization

- Sizing optimization: Find the optimal thickness distribution. The domain is fixed during the optimization.
- Shape optimization: Find the optimal shape. The geometry of the domain is a design parameter. The connectivity of the domain is not changed. New boundaries are not formed.
- Topology optimization: Find the number and location of holes and the optimal placement of material in space.

Scheme of optimization process

Objective function: according to specific applications

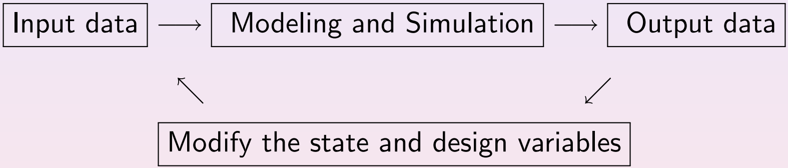

Input/Output data: Physical model; state and design parameters

Modeling and Simulation: e.g., FDM, FEM, FVM

Outline

A general nonlinear optimization problem

$$\min_{\mathbf{x}\in\mathcal{R}^n} f(\mathbf{x})$$

subject to

$$\mathbf{h}(\mathbf{x}) = \mathbf{0}, \qquad \mathbf{g}(\mathbf{x}) \geq \mathbf{0}$$

with twice Lipschitz continuously differentiable functions

$$f : \mathcal{R}^n \to \mathcal{R}, \quad \mathbf{h} : \mathcal{R}^n \to \mathcal{R}^m,\ m < n, \quad \mathbf{g} : \mathcal{R}^n \to \mathcal{R}^\ell.$$

f is referred to the objective (cost) function. The set

$$\mathcal{F} = \{\mathbf{x} \in \mathcal{R}^n :\ \mathbf{h}(\mathbf{x}) = \mathbf{0},\ \mathbf{g}(\mathbf{x}) \geq \mathbf{0}\}$$

is called feasible set. Such problem is called constrained optimization problem. Find a local minimum $\mathbf{x}^* \in \mathcal{F}$, s.t.

$$\exists U \text{ (neighborhood) of } \mathbf{x}^* :\ \forall \mathbf{x} \in U \subset \mathcal{F}, \quad f(\mathbf{x}^*) \leq f(\mathbf{x}).$$

The Lagrangian function $\mathcal{L} : \mathcal{R}^n \times \mathcal{R}^m \times \mathcal{R}^\ell \to \mathcal{R}$ is defined by

$$\mathcal{L}(\mathbf{x}, \mathbf{y}, \mathbf{z}) = f(\mathbf{x}) + \mathbf{y}^T \mathbf{h}(\mathbf{x}) - \mathbf{z}^T \mathbf{g}(\mathbf{x})$$

with $\mathbf{y} \in \mathcal{R}^m$, $\mathbf{z} \in \mathcal{R}^\ell$, Karush–Kuhn–Tucker (KKT) multipliers.

The first–order KKT conditions

1) $\nabla_{\mathbf{x}} \mathcal{L}(\mathbf{x}, \mathbf{y}, \mathbf{z}) = \mathbf{0}$ (stationarity)
2) $\mathbf{h}(\mathbf{x}) = \mathbf{0}$, $\mathbf{g}(\mathbf{x}) \geq \mathbf{0}$ (primal feasibility)
3) $\mathbf{z} \geq \mathbf{0}$, $Z\mathbf{g}(\mathbf{x}) = \mathbf{0}$ (complementarity slackness)

$$\nabla_{\mathbf{x}} \mathcal{L}(\mathbf{x}, \mathbf{y}, \mathbf{z}) = \nabla f(\mathbf{x}) + \sum_{i=1}^{m} y_i \nabla h_i(\mathbf{x}) - \sum_{i=1}^{\ell} z_i \nabla g_i(\mathbf{x}).$$

A point $\mathbf{x}^*$ which satisfies 1)-3) is called a KKT (stationary) point.

Optimization problems with inequality constraints

- Logarithmic barrier functions (a sequence of (BP), $\rho \to 0$)

$$\beta^{(\rho)}(\mathbf{x}) = f(\mathbf{x}) - \rho \sum_{i=1}^{\ell} \log g_i(\mathbf{x}), \qquad g_i(\mathbf{x}) > 0.$$

$$\text{(BP):} \qquad \min_{\mathbf{x} \in \mathcal{R}^n} \beta^{(\rho)}(\mathbf{x}), \quad \text{s.t.} \quad \mathbf{h}(\mathbf{x}) = 0.$$

  $\beta^{(\rho)}$ is the barrier function and $\rho > 0$ is the barrier parameter. The solution points $\mathbf{x}^{(\rho)} \to \mathbf{x}^*$ define the central path.

- Interior–point methods (Karmarkar, 1984)
- Active set strategy

$$\mathcal{A}(\mathbf{x}) = \{i, \; g_i(\mathbf{x}) = 0, \; i = 1, \ldots, \ell\}.$$

Primal–dual interior–point method

$$\mathcal{L}^{(\rho)}(\mathbf{x},\mathbf{y}) = f(\mathbf{x}) - \rho \sum_{i=1}^{\ell} \log g_i(\mathbf{x}) + \mathbf{y}^T \mathbf{h}(\mathbf{x})$$

Consider the following nonlinear equation

$$\mathbf{F}^{(\rho)}(\mathbf{x},\mathbf{y},\mathbf{z}) = \mathbf{0} \quad \text{with} \quad \mathbf{F}^{(\rho)} := \nabla \mathcal{L}^{(\rho)}.$$

3 sets of unknowns: primal variables $\mathbf{x}$, dual variables $\mathbf{y}$, and perturbed complementarity $\mathbf{z}$ with $Z\mathbf{g}(\mathbf{x}) = \rho\,\bar{\mathbf{e}},\ \mathbf{g}(\mathbf{x}) > \mathbf{0}$.

Based on the Newton method we get the primal–dual system

$$K\Delta\mathbf{\Phi} = -\mathbf{F}^{(\rho)}(\mathbf{\Phi})$$

Here, $\mathbf{\Phi} = (\mathbf{x},\mathbf{y},\mathbf{z})^T$ is the unknown solution, $\Delta\mathbf{\Phi}$ is the search direction, $K = (\mathbf{F}^{(\rho)})'(\mathbf{\Phi})$ is the primal–dual matrix.

Path–following predictor–corrector scheme

Predictor step

$$\mu = \rho^{-1},\ \mu \to \infty$$

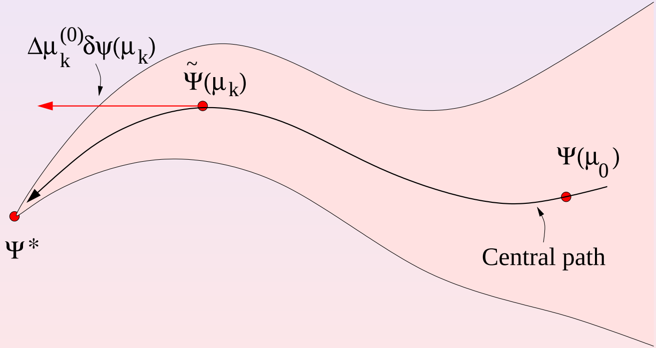

If the solution is out of the contraction tube:

Corrector step: Newton's method

$$\mu = \rho^{-1}, \ \mu \to \infty$$

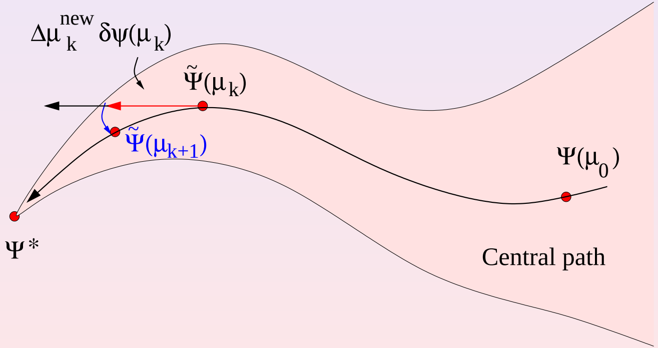

Outline

Biomorphic microstructural ceramic materials

Basic principles of biotemplating: Conversion of bioorganic carbon structures into ceramic composites by high-temperature processing

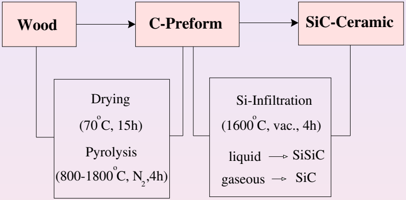

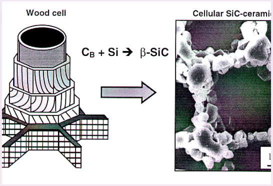

Biopolymers: cellulose, lignin, hemicellulose, pectin, protein

- **Pyrolysis:** the biopolymers are decomposed to carbon. Weight loss: 70-80%, Shrinkage in all directions
- **Infiltration:** liquid (SiSiC ceramics) or gaseous (SiC ceramics)

Silicon Carbide (SiC) ceramic derived from pine

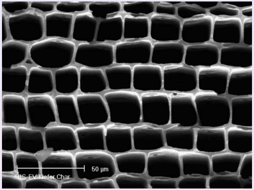

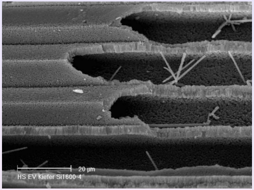

a) radial direction; b) axial direction

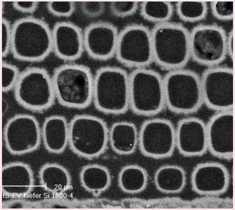

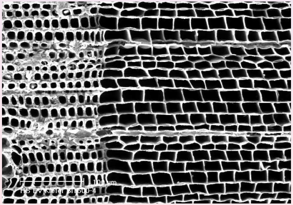

a) C and SiC; b) growing state of wood

Properties and applications

Properties of the SiC–ceramics

- microstructure pseudomorphous to wood
- high strength at low density
- light-weight
- high stiffness and elasticity on micro– and macro–scale
- excellent high temperature stability

Applications of the SiC–ceramics

- acoustic and heat insulation structures
- medical implantation (bone substitution)
- car industry

Macroscopic homogenized material model

Let x – macroscopic, y – microscopic variable, and $\varepsilon := x/y \ll 1$ – scale parameter. When $\varepsilon \to 0$?

Main assumptions:

- Periodic distribution of microcells
- Scale separation: Large gap between micro- and macro-scales!

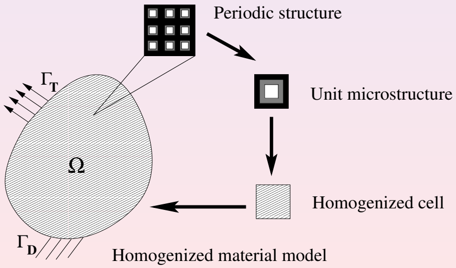

2-D case: Microstructure $Y = [0,1] \times [0,1]$

a) Unit cell $Y = P \cup SiC \cup C$; b) Pure SiC ceramics: $Y = P \cup SiC$

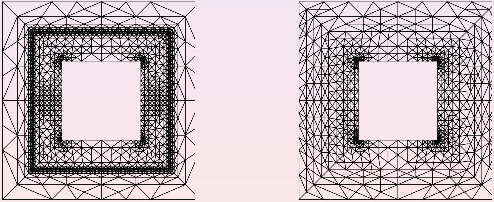

Density $\mu = 84\%$, a) SiC ceramics; b) pure SiC ceramics

Asymptotic homogenization technique

Consider a family of elasticity equations:

$$-\nabla \cdot \boldsymbol{\sigma}_\varepsilon(\mathbf{u}) \;=\; \mathbf{b}(x) \quad \text{in } \Omega \subset R^d,\; d = 2, 3$$

$$\boldsymbol{\sigma}_\varepsilon(\mathbf{u}) := \mathbf{E}_\varepsilon(x)\; \mathbf{e}(\mathbf{u}_\varepsilon) \qquad \text{(Hooke's law)}$$

$$\mathbf{u}_\varepsilon(x) := \mathbf{u}(x/\varepsilon), \qquad \mathbf{E}_\varepsilon(x) := \mathbf{E}(x/\varepsilon) = \mathbf{E}(y).$$

Double scale asymptotic expansion:

$$\mathbf{u}_\varepsilon(x) = \mathbf{u}^{(0)}(x,y) + \varepsilon\, \mathbf{u}^{(1)}(x,y) + \varepsilon^2\, \mathbf{u}^{(2)}(x,y) + \cdots$$

The homogenized problem: $-\nabla \cdot \boldsymbol{\sigma}(\mathbf{u}) = \mathbf{b}(x)$ in Ω,

$$\text{where } \; \boldsymbol{\sigma}(\mathbf{u}) = \mathbf{E}^H\, \mathbf{e}(\mathbf{u}^{(0)}), \;\; \mathbf{u}^{(0)}(x) = \lim_{\varepsilon \to 0} \{\mathbf{u}_{\varepsilon(x)}\}.$$

The homogenized elasticity coefficients

$$E^H_{ijkl} = \frac{1}{|Y|}\int_Y \left(E_{ijkl}(\mathbf{y}) - E_{ijpq}(\mathbf{y})\frac{\partial \xi^{kl}_p}{\partial y_q} \right) \, dY .$$

The Y-periodic function $\xi^{kl} \in [H^1(Y)]^d$ is the solution of

$$\int_Y \left(E_{ijpq}(y)\frac{\partial \xi^{kl}_p}{\partial y_q} \right) \frac{\partial \phi_i}{\partial y_j} \, dY = \int_Y E_{ijkl}(y)\frac{\partial \phi_i}{\partial y_j} \, dY,$$

where $\phi \in \{\psi \in [H^1(Y)]^d, \ \psi \text{ is } Y\text{−periodic}\}$.

$d = 2$ - Solve 3 problems in Y to find $\xi^{11}, \ \xi^{22}, \ \xi^{12}$.

$d = 3$ - Solve 6 problems in Y to find $\xi^{11}, \ \xi^{22}, \ \xi^{33}, \ \xi^{12}, \ \xi^{23}, \ \xi^{13}$.

The shape optimization problem

$$\min_{\mathbf{u},\boldsymbol{\alpha}} J(\mathbf{u},\boldsymbol{\alpha})$$

subject to

$$\sum_{i,j,k,l=1}^{d} \int_\Omega E^H_{ijkl}(\boldsymbol{\alpha}) \frac{\partial u_k}{\partial x_l} \frac{\partial v_i}{\partial x_j} \, d\Omega = \int_\Omega \mathbf{b} \cdot \mathbf{v} \, d\Omega + \int_{\Gamma_T} \mathbf{t} \cdot \mathbf{v} \, d\Gamma$$

$$\sum_{i=1}^{\nu} \alpha_i = C, \qquad \alpha_i^{(\min)} \leq \alpha_i \leq \alpha_i^{(\max)}$$

$\mathbf{u} = (u_i)_{i=1}^N$ are the state parameters, $\boldsymbol{\alpha} = (\alpha_i)_{i=1}^{\nu}$ the design parameters (widths/lengths of layers), and ν the number of layers.

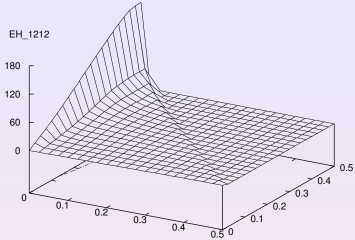

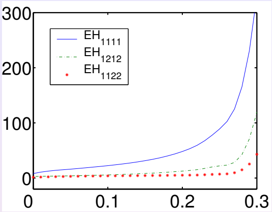

Homogenized coefficients w.r.t. the widths of C/SiC

$\alpha_1^{(0)}$	$\alpha_2^{(0)}$	C	ITER	α_1	α_2	ρ	M	$\lVert \mathbf{F}^{(\rho)} \rVert_2$
0.1	0.1	0.3	11	5.5e-14	0.3	3.0e-14	1.24	1.03e-6
0.2	0.2	0.1	16	5.5e-17	0.1	2.2e-15	7.73	2.23e-8
0.2	0.2	0.2	13	1.0e-16	0.2	5.3e-14	2.34	1.54e-8
0.3	0.1	0.4	11	1.3e-12	0.4	8.5e-13	0.85	5.07e-6
0.4	0.05	0.1	17	9.8e-15	0.1	6.9e-14	7.73	9.49e-7

3–D experiments: Microstructure $Y = [0,1]^3$

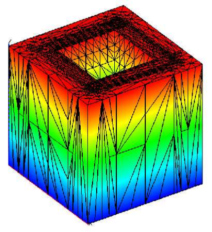

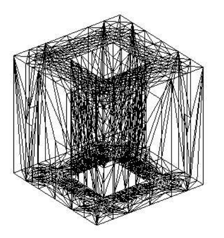

density	level	5	6	7	8	9	10	11
$\mu = 84\%$	NDOF	510	1047	2103	3843	6537	10485	18459
IC	ITER	44	78	117	171	226	273	301
	CPU	0.1	0.6	2.4	8.4	24.3	63.7	187.1
AMG	ITER	18	31	43	73	69	74	75
	CPU	0.4	1.1	3	7.5	15.5	25.6	33.8

Microfluidic biochips

Biochips of microarray type are controllable biochemical labs (lab-on-a-chip) that are used for chemical and biological analysis in pharmacology, molecular biology, and clinical diagnostics.

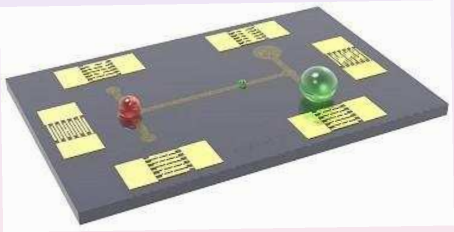

Transport of a droplet containing probe to marker molecules placed on prespecified location. The chip is equipped with paths on which samples and reagents (in amounts of nanoliters) propagate.

Working principles of a SAWs-driven fluidic device

Design of active biochips based on piezoelectrically actuated Surface Acoustic Waves (SAWs) propagating like a miniaturized earthquake. The SAWs are generated by electric pulses of high frequency. The elastic waves interact with the fluid and produce a streaming pattern.

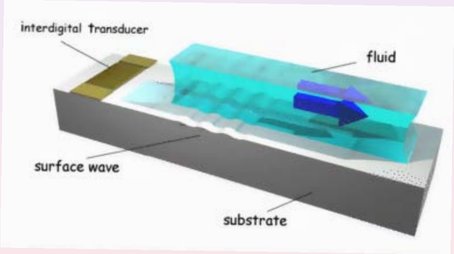

Substrate layer - a piezoelectric material, e.g. lithium niobate.
Interdigital Transducer - fine electrodes with a comb structure.

Optimal design of microfluidic biochips

The efficiency of the labs-on-a-chip essentially depends on their design and production processing

Advalytix Mixer Chip

Our objective function relates:

- geometry of the microchannels
- positioning of the interdigital transducers
- geometry of the capillary barriers and reservoirs.

Modeling of microfluidic flows on biochips

Solve the compressible Navier-Stokes equation in $\Omega(t),\ t > 0$.
Find the velocity $\mathbf{v}$, pressure p, and density ρ such that

$$
\begin{aligned}
\rho\left(\frac{\partial \mathbf{v}}{\partial t} + [\nabla \mathbf{v}]\mathbf{v}\right) &= -\nabla p + \eta \Delta \mathbf{v} + \left(\zeta + \frac{\eta}{3}\right)\nabla(\nabla \cdot \mathbf{v}), \\
\frac{\partial \rho}{\partial t} + \nabla \cdot (\rho \mathbf{v}) &= 0 \qquad \text{continuity eq.} \\
p = p(\rho) &= a\rho^{\gamma} \qquad \text{constitutive eq.}
\end{aligned}
$$

Here, η and ζ are the standard and bulk viscosity and $a, \gamma > 0$.

The Navier-Stokes system is not solved directly due to the extremely different time scales. The acoustic damping is a process with a time parameter in nanoseconds $/10^{-8}s/$ and the acoustic streaming is in milliseconds $/10^{-3} - 10^{0}s/$.

Multiscale modeling based on the approximation theory:

$$
\begin{aligned}
\mathbf{v} &= \mathbf{v}_0 + \mathbf{v}_1 + \mathbf{v}_2 + \cdots = \mathbf{0} + \varepsilon \mathbf{v}' + \varepsilon^2 \mathbf{v}'' + \mathcal{O}(\varepsilon^3) \\
p &= p_0 + p_1 + p_2 + \cdots = p_0 + \varepsilon p' + \varepsilon^2 p'' + \mathcal{O}(\varepsilon^3) \\
\rho &= \rho_0 + \rho_1 + \rho_2 + \cdots = \rho_0 + \varepsilon \rho' + \varepsilon^2 \rho'' + \mathcal{O}(\varepsilon^3)
\end{aligned}
$$

where $\varepsilon,\ 0 < \varepsilon \leq 1$, is proportional to the maximal SAW displacement of the domain boundary. We assume that p_0 and ρ_0 are given constants.

FEM–Simulation by time averaging:

1) acoustic damping equation - collecting all terms of order $\mathcal{O}(\varepsilon)$.

2) acoustic streaming equation - collecting terms of order $\mathcal{O}(\varepsilon^2)$.

PDE constrained optimization problem

Maximize the pumping rate

subject to the PDE constraints on the state variables $\mathbf{v}, p$

$$\begin{aligned} -\nu_1 \Delta \mathbf{v} - \nu_2 \nabla(\nabla \cdot \mathbf{v}) + \nabla p - \mathbf{f}_1 &= 0, \\ \nabla \cdot \mathbf{v} - f_2 &= 0 \qquad \text{in} \;\; \Omega(\boldsymbol{\alpha}) \end{aligned}$$

and the inequality constraints on the design variables $\boldsymbol{\alpha}$.

$$\alpha_i^{\min} < \alpha_i < \alpha_i^{\max}, \qquad 1 \le i \le k.$$

Here, k is the number of Bézier control points.

Ω includes a capillary barrier, reservoir, and outlet valves. The valves are passive when the capillary barrier is opened and activate when it is in stopping mode.

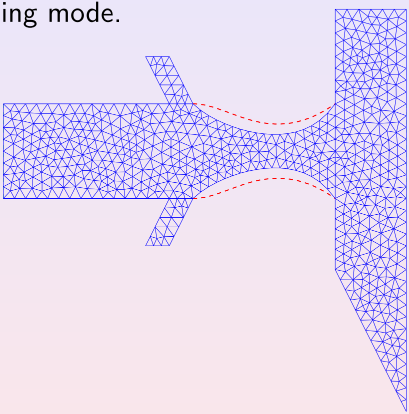

Design–Variables: Bézier control points

N - d.o.f., I - Newton's iterations, $tol = 10^{-4}$ - tolerance in the continuation method, $tol_n = 10^{-3}$ - tolerance of the inexact Newton solver, μ - inverse barrier parameter ($\mu_0 = 200$), $\Delta\mu$ - its increment ($\Delta_{\mu_0} = 500$), θ - contraction factor in the monotonicity

N	k	I	μ	$\Delta\mu$	θ
14240	0	-	2.0 e+2	5.0 e+2	-
	1	2	2.0 e+2	4.8 e+2	0.35
	2	1	1.38 e+3	2.1 e+3	0.07
	3	1	4.23 e+4	3.5 e+3	0.48

N	k	I	μ	$\Delta\mu$	θ
28524	0	-	2.0 e+2	5.0 e+2	-
	1	3	2.0 e+2	4.6 e+2	0.23
	2	2	4.35 e+3	3.2 e+3	0.18
	3	1	5.27 e+4	7.3 e+3	0.56

Table: Convergence results of the path-following method

Outline

Optimal design

Optimization problem and solution methods

Multiscale shape optimization problems

- Microstructural ceramic materials
- Microfluidic biochips

Conclusions

Conclusions

- Discrete models for the specific applications
- Homogenization techniques in 2D and 3D
- Adaptive grid refinement, a posteriori error estimators
- Optimization problem with PDE constraints
- Multiscale algorithms
- Primal–dual interior–point methods
- Path–following predictor–corrector scheme

Acknowledgements: DFG SPP 1253, DAAD PPP